An experimental study on the influence of composite materials used to reinforce masonry ring beams

Romina SISTI
Department of Engineering, University of Perugia
Via Duranti, 93 06125 Perugia, Italy

Marco CORRADI
Corresponding author,
Mechanical and Construction Engineering Department, Northumbria University Wynne-Jones Building, NE1 8ST, Newcastle upon Tyne, United Kingdom and Department of Engineering, University of Perugia, Via Duranti, 93 06125 Perugia, Italy
email marco.corradi@northumbria.ac.uk
Tel. +44 (0) 191 243 7649, Fax. +44 (0) 191 227 4561

Antonio BORRI
Department of Engineering, University of Perugia
Via Duranti, 93 06125 Perugia, Italy

HIGHLIGHTS

We carried out bending tests on 10 full-scale composite-reinforced masonry ring-beams.

Ring beams were rinforced with different composite materials embedded into an inorganic matrix.

GFRP grids, glassfibre nets and PBO cords have been used to reinforce the masonry beams. Reinforced ring beams presented enhanced behavior and increased mechanical properties.

Keywords: masonry, mechanical testing, composite materials, earthquake engineering

ABSTRACT: For historic masonry constructions the out-of-plane wall behavior is critical to seismic performance. Because the main cause of out-of-plane collapses is the wall-to-wall level of connection, the application of a Reinforced Concrete (RC) ring beam at the eaves level of historic masonry buildings is an effective method to prevent an out-of-plane mechanism of a wall panel. However this effective reinforcing method presents some drawbacks. In order to address this, this paper describes the problems associated with this "traditional" reinforcing method and introduces a new retrofitting technique for historic masonry buildings by realizing a new type of ring beam made of recycled old stones or bricks reinforced at the bed joints with glass-fibre sheets, GFRP (Glass Fiber Reinforced Polymer) grids or/and PBO (polybenzoxazole: poly-p-phenylene benzobisoxazole) cords. An experimental investigation has been carried out on 10 full-scale rubble-stone or brickwork masonry ring beams. The testing included the use of composite materials inserted into the mortar joints during the fabrication phase of the beams and pinned end conditions (four-point bending configuration). Beams were reinforced with different composite layouts.

INTRODUCION

The estimation of the strength of a masonry construction is based on the analysis of the modes of failure and several theories have been developed which are able to predict the type, direction and magnitude of loading which will produce the failure in that mode.

Masonry constructions tend to lack connections between walls and between walls and floors. Most traditional typologies of historic construction have roof and floors which span only one way and in case of a seismic event the transfer of the horizontal loads from these horizontal structural elements into the walls is often critical.

In order to achieve unitary behaviour of the structure against earthquakes, these constructions must be upgraded so that they avoid local collapse and have integrating structural elements. Because of the wall-to-roof connection is often considered as the principal critical element, several solutions have been proposed in the past. For example, improvement has been achieved by tie rods or ring beams. In old buildings, it is often possible to find wooden/metal ties and connectors inside masonry [1-2]. In the 70s and 80s of last century, wood beam floors have been replaced with RC ring beams (Fig. 1) [3-5] or with heavy two-ways RC roofs and floors. Stiff diaphragm-like floors are desirable structurally but require the dismantling of old two-ways spanning wooden floors.

During 1998 to 2011 a series of experiments were carried out at several laboratories in Italy, France, Greece, Portugal and Slovenia to asses a range of different reinforcing methods for historic masonry. A growing awareness amongst researchers and engineers of the importance of the mechanical properties of FRP (*Fiber Reinforced Polymer*) have produced interesting structural solutions for the rehabilitation of existing masonry constructions.

Recent earthquakes have shown the limitations of new and more conventional techniques. For example the installation of RC ring beams has proved to be ineffective or to increase the seismic vulnerability of the construction when inadequately designed, not well connected to the existing masonry, when used on a poor masonry or in combination with heavy RC floors. It has been recognized by now that the greater stiffness of the RC ring beam compared to the stiffness of the masonry, produces a different response in these two materials during earth-quakes and causes the load to be unevenly spread. In order to prevent out-of-plane collapse

74 mechanisms, the action of vertical static loads may contribute to stabilize wall panels, but the
75 application of stiff RC ring beam may cause the re-distribution of vertical compressive stress-
76 es and some portions of masonry could results unloaded and, during earthquakes, be prone to
77 become unstable (Fig. 2) [6-8].
78 Nowadays, it's usual to apply steel-profiles or masonry ring beams (Figs. 3-4). However,
79 when a building is faced with stone, ring beams are made thinner than the wall so that they are
80 screened and remain invisible on the façade. This kind of reinforcement is impossible when
81 the thickness of the wall is small and it introduces an element which is extraneous to the exist-
82 ing structure.
83 Recently researchers have focused their interest on the use of composite materials coupled
84 with non-polymeric matrixes [9-14], like lime-based mortars [15-18] with the aim at increas-
85 ing the durability [19-20]. The aim is to avoid the use of epoxy or other polymeric resins, due
86 to their critical long-term behavior. In this area, the new reinforced masonry ring beam pro-
87 posed in this paper is based on the aspiration to use existing materials (stones or bricks), with
88 a composite reinforcement embedded into the mortar bed joints. This retrofitting method re-
89 quires the demolition of a small portion of the walls. These are then reconstructed, using re-
90 covered stones and hydraulic mortar reinforced with composite materials. The use of compo-
91 site materials with non-organic matrices has been recently investigated [21-24].
92 It is known that the tensile strength of brick-masonry or perfectly-cut stonemasonry, character-
93 ized by horizontal mortar bed joints and staggered vertical joints, is governed by the friction
94 coefficient between blocks and mortar (Fig. 5), whereas for random rubble stone masonry this
95 relies only on the mortar tensile strength [25]. In the past, with the aim at increasing the ma-
96 sonry tensile strength, random rubble stonemasonry was often reinforced with wooden beams
97 embedded into the walls during the construction, as reported by Giuffrè [25]. The resistance of
98 these elements to sliding is due to the winding shape of the beams rather than the adhesion be-

tween wood and mortar, and for this reason the resistance is nondependent of the compression stress in the masonry.

The retrofitting method proposed in this paper is inspired by the technique mentioned above: the wooden beams are replaced with composite nets or grids (Fig. 6). The authors have already investigated in the past a similar solution, applied only to brickmasory, using fiberglass sheets or steel cords [26-27] embedded into a cementitious grout. In this paper this retrofitting method has been adapted to random rubble stone masonry, using also non-cement based mortars.

EXPERIMENTAL WORK

Description of specimens

Ten masonry beams were constructed and subjected to bending test, eight from stones and two from solid clay bricks. Specimens have a letter designation (P and L for stone and clay beams, respectively) followed by an identification number from 1 to 10. The tests were not designed to simulate exactly an earthquake dynamic loading but to generate a set of internal forces in the ring beam similar to those which would be induced by both the vertical and horizontal action of the seismic loading. Masonry ring beams were loaded statically to failure. These specimens were tested by applying the bending load perpendicularly and parallel to the mortar bend joints and reinforcement sheet/grid (Fig. 7) in order to simulate an in-plane vertical and out-of-plane horizontal seismic action, respectively.

Stonemasonry specimens were based upon a 5 m length and a cross-section of 0.5 x 0.5 m. Beams were formed by 3 layers of stones and 4 layers of composite reinforcement. The ready-to-use hydraulic CM lime-mortar was used for the construction of these panels (Tab. 1).

Brickmasonry specimens had the dimensions of 0.4 x 0.33 x 5 m (width x height x length) and were constituted by 4 and 5 layers of bricks and composite reinforcement, respectively (Fig.

8). Different composite materials were used as reinforcement. Two stonemasonry beams (P1 and P2) were strengthened with 4 glass fiber mesh sheets (5.0 x 0.5 m) and 8 twisted PBO (1,4-benzene dicarboxylic acid, polymer with 4,6-diamino-1, 3- benzenediol dihydrochloride) cords (Figs. 9-10a). For each layer of composite reinforcement, 1 mesh sheet and 2 PBO cords were used. PBO cords were passed through and interwoven in the glass-fibre mesh at a distance of approx. 5 cm from the lateral beam sides.

Two further specimens (P3 and P4) were reinforced using the same glass-fibre mesh sheet, but a different type of PBO cords. In this case ropes were constituted of an unidirectional PBO fiber core and a protection cover of PET (polyethylene terephthalate) (Fig. 10b). For these specimens the reinforcement arrangement is similar to the one previously used (4 glass sheets and 8 PBO cords).

Ring beams P5, P6, P7 and P8 were reinforced using 4 GFRP grids (grid dimension 0.5 x 5 m), made of AR (Alkali-Resistant) glass and of thermosetting epoxy vinyl ester resin. GFRP grids have different mesh size: rigid square meshes sized 33x33 mm were used in samples P5 and P6, whereas a mesh size of 66x66 mm has been applied for P7 and P8 samples (Fig. 11). The remaining two samples were made of brickwork masonry. These ring beams had the same length (5 m) but different cross-section (0.40 x 0.33 m). Brickwork beams were made of 4 courses of hollow bricks and 5 layers of composite reinforcement (Fig. 12). The grout used for the beam construction was the ready-to-use cement-based MI mortar (Tab. 1).

Each bending test is identified with a designation of three indices, the first indicates the masonry material (P and L, for stone- and brick-masonry, respectively) and the beam's identification number (for example P4 indicates the stonemasonry ring beam No. 4), the second the type of strengthening (T = fiberglass sheet and PBO cord with twisted configuration, U = fiberglass mesh and PBO cord with unidirectional core, G33 = GFRP grid with a mesh size of 33 x 33 mm; G66 = GFRP grid with a mesh size of 66 x 66 mm) and the last one the direction of the

bending loads with regard to the mortar bed-joints (V or H for bending loads parallel or perpendicular to the mortar bed joints, respectively).

During the construction, the specimens were confined using wooden scaffoldings which were removed before the bending tests. Tests were conducted over a span of 4 m and the beam's ends rested on two 0.5x0.5x0.25 m concrete blocks.

Characterization of materials

Mortars

Two types of mortar have been used to construct the masonry beams. The strength of the two mortars was determined by compression tests on cylindrical samples approx. 95 mm in diameter and 190 mm in height according to UNI EN 12390-3 [28]. During the construction of the ring-beams, two or three mortar specimens have been casted for each beam. Test results are reported in Table 1. The letter designations CM and MI were used to identify the mortars. Mortar CM is a lime-based mortar while MI is cement-based. Stone- and brick-masonry beams were assembled using CM and MI type, respectively. 23 compression tests were conducted on the mortars: the mean value of the compressive strength was 5.99 (Coefficient of Variation (CoV) 9.56%) and 10.61 MPa (CoV = 6.32%), for mortar CM and MI, respectively.

Stones and bricks

Compression tests using a 1000 kN Metrocom Engineering press were also conducted on 6 prismatic stone specimens (dimensions 50 x 50 x 70 mm). The specimens were made of a white-colored calcareous stones with a weight density of 2520 kg/m^3 , obtained from an old building seriously damaged during the 2009 L'Aquila earthquake. UNI EN 1926 [29] standard was adopted for test conditions. Compressive strength was 24.42 MPa and the coefficients of

variation for both weight density and strength were very limited (3.68 and 8.94%, respectively).

L9 and L10 beams were assembled using hollow clay bricks (dimensions: 55 x 120 x 250 mm) with a 36% of void area. Compression tests on five bricks in the direction parallel to the holes gave a strength of 46.33 MPa; while this was 11.53 MPa in the perpendicular to the hole direction.

PBO cords

The cords used to reinforce the first four samples were made of PBO fibers, commercially known as Zylon. This material was selected for its high Young's modulus and tensile strength. It also presents good creep resistance.

Two kinds of cord have been used as reinforcement: types T, with a twisted configuration, and U, with a unidirectional fiber core. Table 2 summarizes the results obtained from tensile tests carried out in accordance with ASTM D2256 [30] standard.

The tensile strengths of the two types of cord are similar whereas the Young's modulus of U cord is higher than the T one. Elongation at failure is1.07% for U cord and 3.22% for T cord, respectively.

GFRP sheet

The glass prepreg fiber sheet is made of a square mesh with nominal dimensions of 12x12 mm. In both directions there are 0.48 mm^2/cm of fiberglass and the failure load is 70 kN/m. The roving is an AR-glass (Alkali-Resistant). Table 3 gives the GFRP mechanical properties.

GFRP grids

The GFRP is made up of continuous fiber filaments embedded in thermosetting epoxy vinyl ester resin matrix. Two mesh sizes were used in the investigation: 66 x 66 and 33 x 33 mm. Specimens of multiple twisted warp and weft direction were extracted and mechanical characteristics were analyzed via tensile tests. Test results are shown in Table 4.

Test procedure

The beams were simply supported at the ends over a span of 4 m. Bending load was uniformly distributed along 2 m (Fig. 13). Linear Variable Differential Transducers (LVDTs) were placed at ¼ , ½ and ¾ of beam's span to measure vertical deflections. When cracks appeared just for the weight of the beam itself, the displacements were measured manually with a millimetric sensitivity of measurements.

Figure 14 shows the testing arrangement for a brickwork beam for both loading conditions (perpendicular and parallel to the mortar joints) . In order to bend the beams in their horizontal plane and simulate the seismic action, some specimens were confined with wooden planks and webbings clamped with ratchets and then were rotated 90°. After this rotation the load was spread on the upper surface.

The bending load was applied to the beams using concrete blocks and/or cement bags. The possibility of the beam twisting has been taken into account by applying LVDTs on both sides of the beams. Small differences in LVTDs readings demonstrate that there was negligible twisting.

Test results and analysis

Because historic masonry has high compressive strength but has also very low tensile strength unless reinforced, it was not possible to construct unreinforced specimens to compare results. Taking the beam self-weight into consideration, this can easily generate a stress on the beam's

tension side much higher than the masonry tensile strength. A masonry beam with the dimensions used in this investigation cannot stand alone over a span of 4 m, especially when it is made using a weak lime-based mortar.

When stressed with bending and shear loads, historic masonry behaviour is often dominated by the mechanical properties of the lime-based mortar and mainly by its tensile strength. This is in the range 0.002-0.05 MPa [31-32]. Also considering the upper bound value, for a 0.5x0.5x5 m beam tested in 3-point bending over a span of 4 m, this corresponds to a bending load of 10.4 kN (1020 kg) compared to an approximate self-weight of 2375 kg for a stonemasonry beam with these dimensions.

Table 5 shows the cross sectional areas of composite material used to reinforce both stone- and brickmasonry beams. Results of all tests are presented in Table 6. In this table maximum mid-span bending moments produced by both self-weight (M_w) and by external loads (M_{Load}) are listed. The bending moment produced by the self-weight has been obtained from the masonry weight density. This was 2140 and 1464 kg/m^3 for stone- and brick-masonry beams, respectively.

With regard to the specimens reinforced using PBO cords and fiberglass sheets, the P1-T-V sample was bended perpendicularly to the bed joints plane and the load was applied in increasing steps of 0.1 kN, stacking cement bags. When the bending load reached the value of 16 kN, suddenly two vertical cracks formed in the mortar joints, 1.97 m from the nearest support, and the specimen leaned on the ground. The total mid-span bending moment was 22.47 kNm.

For P2-T-H, P3-U-V and P4-U-H specimens, initial cracking appeared from the beginning near beam mid-span as result of self-weight loads when the wooden scaffoldings were dismantled. However the beam did not collapse and it was possible to apply a further bending load. This initial cracking was caused by a progressive tensile failure of the fiberglass sheet,

247 whereas the PBO cords were not damaged (Fig. 15a). The variation in bending stiffness indi-
248 cated a shift from an elastic behavior (in which all the materials act as one) to a plastic one (in
249 which only the PBO cords provide the needed tensile strength to the beam). By increasing the
250 bending load, the deflection of the beams increased considerably until failure; it is noteworthy
251 to mention that the tensile failure of PBO cords was never reached (Fig. 15b). Debonding of
252 the composite reinforcement (glass-fiber sheet and PBO cords) and mortar cracking were the
253 main cause of the ring-beam's collapse.
254 The different PBO cords used to reinforce P1 and P3 stonemasonry beams (both loaded paral-
255 lel to the mortar bed joints with a similar reinforcement arrangement) did not significantly af-
256 fect the beam bending capacity (Tab. 1). In terms of maximum mid-span bending moment the
257 difference between the results is smaller than 6 %. For P1-T-V sample twisted PBO cords
258 were used while unidirectional ones were adopted for P3-U-V. The different type of the PBO
259 cords did not affect the response: the rougher surface of the twisted cords used in P1-T-V test
260 did not facilitate the adhesion with the inorganic matrix (the mortar).
261 With regard to the specimens reinforced using GFRP grids (P5, P6, P7, P8, P9 and P10), the
262 overall capacity of the ring-beams was significantly higher compare the one measured for
263 specimens reinforced with PBO cords and fiberglass sheets. The maximum mid-span bending
264 moment increased to 48.35 kNm from 21.44 kNm measured for beams previously tested. The
265 6 simply-supported specimens that had failure initiating at mid-span had similar longitudinal
266 and transverse strain gradients prior to failure. For a load of 21 kN, specimen P5-G33-V ex-
267 hibited vertical cracks on both the lateral vertical surfaces. By increasing the load magnitude,
268 the ring beam underwent a progressive degradation: the number of vertical cracks amplified
269 and horizontal crack at the bed joints opened near the beam's ends (Fig. 16). At beam's mid-
270 span, diagonal cracks also opened and composite partially separated from the mortar. The ca-
271 pacity of the beam was 56.8 kN.

Test P8-G66-H exhibits vertical cracks at mid-span for a load of 10.5 kN. The maximum load applied on this ring-beam was 43.1 kN. For this load level many vertical cracks opened at beam intrados (Fig. 17). However it was not possible to take the specimen to failure for the difficulty in the application of the external load.

With regard to test L9-G33-V, for a load level of 14.6 kN, several vertical cracks opened at mid-span. By increasing the magnitude of the vertical load, cracks spread toward beam extrados. Again, composite detached from the its matrix (the mortar) at the joint between the first/second and second/third course of bricks.

For L10-G33-H test, the maximum external load applied was 38.3 kN. Test was stopped at this level of load without having reached the failure of the masonry beam.

For all bending tests, diagrams of vertical deflections vs. position have been plotted in such a way that it is possible to appreciate the deformed configuration of the masonry beam. Figure 18 shows this curves at different load levels for test L10-G33-H.

Figure 19 shows the moment-curvature response for all bending tests. In this graph, the calculation of the bending moments was made by considering the applied external load and neglecting the contribution of the self-weight. The curvature is given in terms of beam rotation at the end supports. Figure 19 only shows the last cycle of loading: tests No. L10-G33-H and P6-G66-H present a residual deformation produced during the previous loading phase.

Following the flexure test, an undamaged beam's portion was tested in compression in order to find the masonry compressive strength and Young's modulus. The load was generated by means of two 1000 kN hydraulic jacks, distributed to an area of 0.5 x 0.5 m using a 14 mm-thick steel plate. The eight of the masonry specimens was approx. 0.5 m. Three LVDTs were applied to measure the vertical displacements in compression. Failure occurred at the stone-mortar interface (typically shear and tensile modes) with limited or no damage on the stones.

The behavior of the masonry material was highly dominated by the mortar's mechanical prop-

297 erties. Results show an average stonemasonry compressive strength and a Young's modulus of
298 3.63 and 4458 MPa, respectively. The stonemasonry Young's modulus was calculated from
299 the slope of the load-deformation curve (using the compressive stress at 10% and 40% of the
300 masonry strength). Figure 20 shows the compressive load –deflection plot. Masonry response
301 can be approximated to an ideal elastic-plastic model with an ultimate deformation of 3.5‰.
302
303 COMPARISON BETWEEN ANALYTICAL PREDICTIONS AND TESTS RESULTS
304 A simplified method, based on the beam's theory, was used to calculate the mid-span (maxi-
305 mum) bending moment at failure. The ultimate bending moment of each beam was calculated
306 on the basis of the following assumptions: linear strain diagram (plane cross section remaining
307 plane); perfect bond between masonry and reinforcing composite materials; negligible tensile
308 strength of masonry, reinforcing materials being non-reactive in compression (Fig. 21).
309 The stress-strain relationship of stone masonry is assumed to be similar to the bilinear curve
310 obtained from the compression test (Fig. 20); while a brickmasonry compressive strength and
311 Young's modulus (equal to 11 MPa and 11.04 GPa, respectively) were evaluated using the
312 Italian building code [33].
313 Maximum mid-span moments were calculated using the analytical method and compared with
314 experimental values. Results are summarized for all the beam tests in Table 7. A good agree-
315 ment can be noted between the analytical calculation and experimental results in terms of
316 maximum bending moment. However for the first four tests (from P1 to P4), results signifi-
317 cantly diverged: this is probably due to the fact that the beam's self-weight caused the failure
318 of the fibreglass net and the bonding between the fibre and the mortar. This highly reduced the
319 beam bending capacity. By increasing the bending loads, only the PBO cords effectively acted
320 to resist, while analytical values have been calculated by considering both fibreglass net and
321 PBO cord contribution and this leaded to an overestimation of the beam capacity.

CONCLUSIONS

This research has demonstrated that it is possible to use composite materials coupled with inorganic cement-based matrices to construct masonry ring beams. This could be an interesting alternative to the use of traditional heavy and stiff reinforced concrete beams for restoration and upgrading interventions on historic masonry structures. The reinforcing method consists in the construction of a stone- or brick-masonry ring beam at the roof level using recycled or new stones/bricks. This is also of interest when fair-faced masonry is a particular requirement for a historic building. The reinforcement method allows to keep the masonry fair faced appearance and composite reinforcement is completely embedded into the horizontal mortar bed joints.

A series of flexure tests were experimentally examined to help develop estimates of their flexural capacity in both planes parallel and perpendicular to the mortar bed-joints. Two different materials (stones and bricks) and three types of composites (fiberglass sheets, GFRP grids and PBO cords) were studied and used as reinforcement. All specimens were tested in four point bend with simply-supported end conditions.

Mid-span maximum moments at failure were estimated using linear methods based on basic beam theory. Examining the calculated moment magnitudes, findings from the study indicated that:

1) Four tests have been carried out on stonemasonry beams reinforced using GFRP grids and PBO cords. Results demonstrated that the reinforced beams are able to resist high bending loads only after the initial cracking in the mortar.

2) During the bending tests, the PBO cords never failed in tension, but by increasing the bending load, beam’s vertical deflections and crack widths in the mortar bed-joints became very large. The bonding between the PBO cord and its matrix (the mortar) was weak and this par-

tially prejudiced the resisting action of the PBO cords. Only when the ring-beam's vertical deflections reached high levels, the contribution of PBO cords was activated.

3) Reinforcement was more effective when GFRP grids were used (tests P5, P8, L9 and L10). Results of the last four tests evidenced high values in terms of capacity loads and bonding characteristics between GFRP and mortar. For these tests, the analytical calculations of the maximum bending moment was in good agreement with experimental findings.

4) For beams reinforced with GFRP grids, the bending capacity was very high for all tests performed in both planes parallel and perpendicular to the mortar bed-joints.

ACKNOWLEDGEMENTS

The authors express their gratitude to Tecnoclima Group s.r.l. for manufacturing facilities provided. This project was sponsored by the Italian Ministry of Education [ReLUIS (2014) Linea di ricerca WP1 e WP2]. The authors acknowledge Fibre Net S.r.l. for providing the composite materials. The authors also thank Alessio Molinari, Mattia Procacci, Ilenia Rinchi and Alessio Di Mauro.

REFERENCES

[1] Spence R, Coburn A. Strengthening buildings of stone masonry to resist earthquakes. In Masonry Construction (pp. 213-221). Springer Netherlands, 1992.

[2] Frumento S, Giovinazzi S, Lagomarsino S, Podestà, S. Seismic retrofitting of unreinforced masonry buildings in Italy, Proceedings of New Zealand Conference for Earthquake Engineering, March, 10-12, 2006.

[3] Penazzi D, Valluzzi MR, Saisi A, Binda L, Modena C. Repair and strengthening of historic masonry buildings in seismic areas. Proceeding of International congress, more than two thousand years in the history of architecture, Bethlehem, Palestine, September 10-12, 2001.

[4] D'Ayala D, Speranza E. Definition of collapse mechanisms and seismic vulnerability of historic masonry buildings. Earthquake Spectra 2003;19(3):479-509.

[5] Alexandris A, Protopapa E, Psycharis I. Collapse mechanisms of masonry buildings derived by the distinct element method. Proceedings of the 13th world conference on earthquake engineering, 2004.

[6] Binda L, Gambarotta L, Lagomarsino S, Modena C. A multilevel approach to the damage assessment and seismic improvement of masonry buildings in Italy. Seismic damage to masonry buildings. Balkema, Rotterdam, 1999;170-195.

[7] Furukawa A, Ohta Y. Failure process of masonry buildings during earthquake and associated casualty risk evaluation. Natural hazards 2009;49(1),25-51.

[8] Magenes G, Penna A, Senaldi IE, Rota M, Galasco A. Shaking Table Test of a Strengthened Full-Scale Stone Masonry Building with Flexible Diaphragms. Int J Archit Heritage 2014;8(3):349-375.

[9] Huang X, Birman V, Nanni A, Tunis G. Properties and potential for application of steel reinforced polymer and steel reinforced grout composites. Compos Part B 2005; 36:73–82.

[10] Prota A, Marcari G, Fabbrocino G, Manfredi G, Aldea C. Experimental in-plane behavior of tuff masonry strengthened with cementitious matrix–grid composites. J Compos Constr 2006;10(3):223-233.

[11] Corradi M, Borri A, Vignoli A. Experimental evaluation of the in-plane shear behaviour of masonry walls retrofitted using conventional and innovative methods. Masonry Int 2008;21(1):29-42.

[12] Papanicolaou CG, Triantafillou TC, Papathanasiou M, Karlos K. Textile reinforced mortar (TRM) versus FRP as strengthening material of URM walls: out-of-plane cyclic loading. Mater Struct 2008;41:143–157.

[13] Gattesco N, Dudine A. Effectiveness of masonry strengthening technique made with a plaster reinforced with a GFRP net. Proceedings 8th International Masonry Conference 5-9 July 2010, Dresden, Germany.

[14] Castori G, Borri A, Corradi M. Behavior of thin masonry arches repaired using composite materials. Compos part B 2015;87:311–321.

[15] Borri A, Castori G, Corradi M, Sisti R. Masonry wall panels with GFRP and steel-cord strengthening subjected to cyclic shear: an experimental study. Constr Build Mater 2014;56:63-73.

[16] De Felice G, De Santis S, Garmendia L, Ghiassi B, Larrinaga P, Lourenço PB, Oliveira DV, Paolacci F, Papanicolaou CG. Mortar-based systems for externally bonded strengthening of masonry. Mater Struct 2014; 47:2021-2037.

[17] Razavizadeh A, Ghiassi B, Oliveira DV. Bond behavior of SRG-strengthened masonry units: Testing and numerical modeling. Constr Build Mater 2014; 64:387-397.

[18] De Santis S, de Felice G. Tensile behaviour of mortar-based composites for externally bonded reinforcement systems. Compos part B 2015; 68:401-413.

[19] Carpinteri A, Grazzini A, Lacidogna G, Manuello A. Durability evaluation of reinforced masonry by fatigue tests and acoustic emission technique. Structural Control & Health Monitoring, 2014; 21: 950- 961.

[20] Carpinteri A, Lacidogna G, Paggi M. Acoustic emission monitoring and numerical modeling of FRP delamination in RC beams with non-rectangular cross-section. Materials and Structures, 2007; 40: 553-566.

[21] Ascione L, de Felice G, De Santis S. A qualification method for externally bonded Fibre Reinforced Cementitious Matrix (FRCM) strengthening systems. Compos part B 2015;78:497-506.

420 [22] Tumialan JG, Micelli F, Nanni A. Strengthening of masonry structures with FRP compo-
421 sites. Proceedings of Structures 2001, Washington DC, May 21-23, 2001.
422 [23] Roca P, Araiza G. Shear response of brick masonry small assemblages strengthened with
423 bonded FRP laminates for in-plane reinforcement. Constr Build Mater 2010;24(8): 1372-
424 1384.
425 [24] Corradi M, Borri A, Castori G, Sisti R. Shear strengthening of wall panels through jack-
426 eting with cement mortar reinforced by GFRP grids. Compos Part B 2014;64: 33-42.
427 [25] Giuffrè A. Seismic damage in historic town centres and attenuation criteria. 1995.
428 [26] Borri A, Castori G, Grazini A. Retrofitting of masonry building with reinforced masonry
429 ring-beam. Constr Build Mater 2009;23(5):1892-1901.
430 [27] Borri A, Sisti R, Corradi M. Experimental analysis of stone-masonry ring beams rein-
431 forced with composite materials. Proceedings 6th IB2MAC, Padova, Italy, June 26-30,
432 2016.
433 [28] UNI EN 12390-3 2009. Testing hardened concrete, Part 3: Compressive strength of test
434 specimens.
435 [29] UNI EN 1926 2007. Natural stone test methods – Determination of uniaxial compressive
436 strength.
437 [30] ASTM D2256 2002. Standard test method for tensile properties of yarns by the single-
438 strand method.
439 [31] Silva BA, Pinto AF, Gomes A. Influence of natural hydraulic lime content on the proper-
440 ties of aerial lime-based mortars. Constr Build Mater 2014;72:208-218.
441 [32] Cangi G. Manuale del recupero strutturale e antisismico. 2012, Ed. DEI, Rome [in
442 Italian].
443 [33] Italian Ministry of Infrastructures, 2008, Italian Construction Code: Norme Tecniche per
444 le Costruzioni, 2008.

445

Figure 1. Example of a RC ring-beam.

Figure 2. Examples of an out-of-plane collapse due to poor connection between the RC ring beam and the underlying masonry.

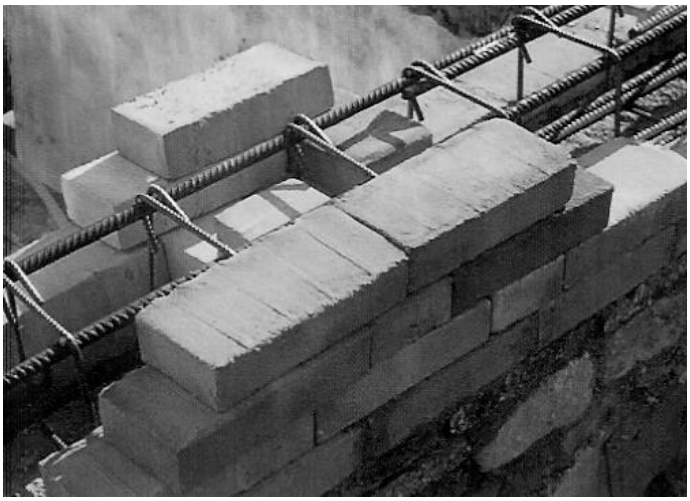

Figure 3. Example of a brickwork steel-reinforced ring-beam.

Figure 4. Example of a steel-profile ring-beam.

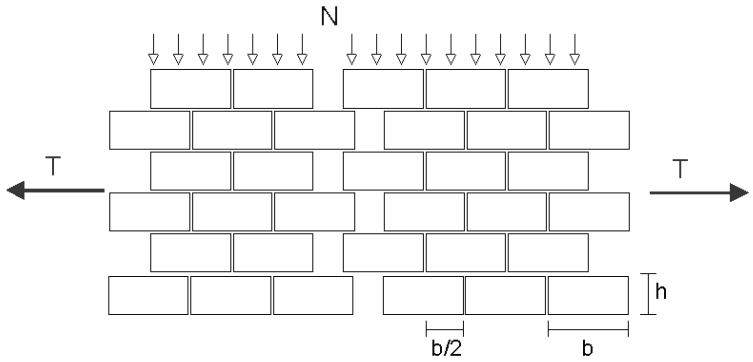

Figure 5. The response of a wall with regular horizontal bed mortar joints to horizontal tensile loading [32].

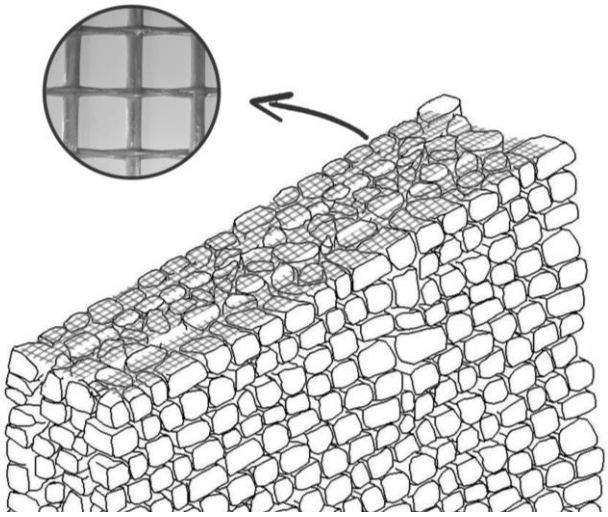

Figure 6. Application of a GFRP grid/ glass fiber sheet inside the horizontal mortar joint.

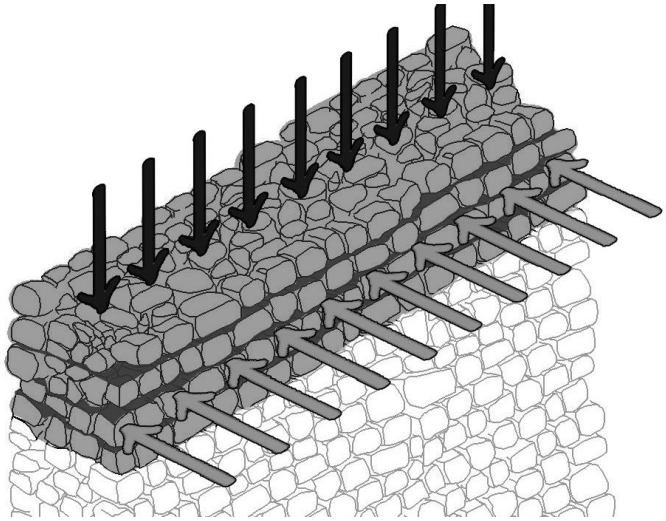

Figure 7. Ring beams were tests both parallel and perpendicular to the reinforcement.

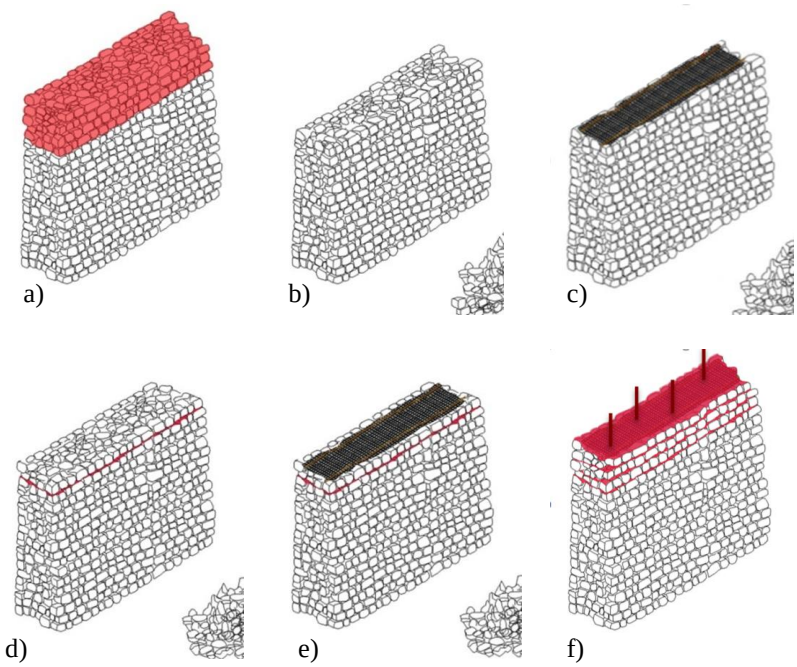

Figure 8. Construction methods of a reinforced masonry ring beam: a-b) taking down the upper part of the wall; c) laying out the first mortar bed reinforced with the composite; d) laying the stones; e) spreading the second layer of reinforced mortar; f) repeating the phases d)-e) until reaching the required height.

552

553

554

555

556

557

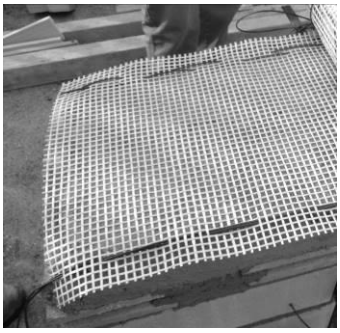

a)

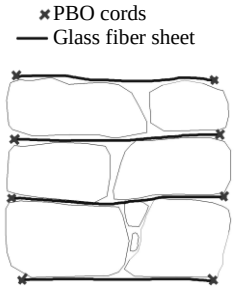

b)

558

559 Figure 9. Construction of stone ring-beam strengthened with glass fiber sheets and PBO cords: a) ax-

560 onometric view, b) beam's cross section.

561

562

563

564

565


a)

b)

567 Figure 10. The cords used to reinforce the samples: a) twisted PBO cord, b) PBO cord with unidirec-

568 tional core.

569

570

571

572


a)

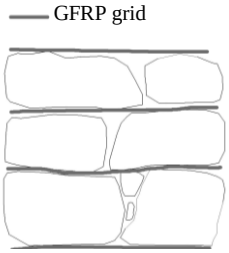

b)

573

574 Figure 11. Construction of stone ring-beam strengthened with GFRP grids: a) lateral view,

575 b) beam’s cross section.

576

a)

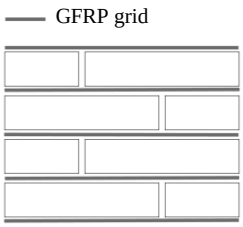

b)

Figure 12. Construction of brickwork ring-beam using a GFRP grid: a) axonometric view, b) beam's cross section.

586

587

588

589

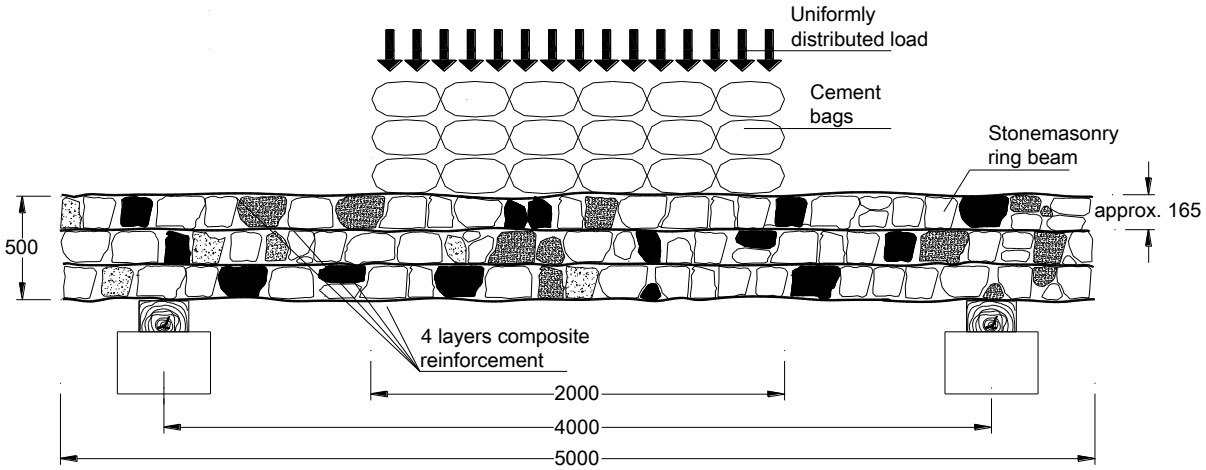

590

591 Figure 13. Arrangement of bending test of stonemasonry ring beams (dimensions in mm).

592

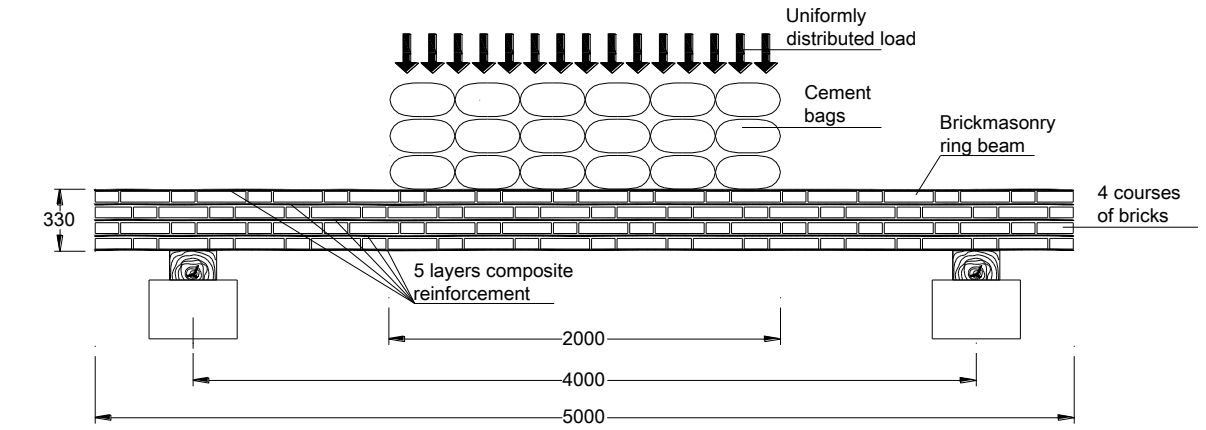

a)

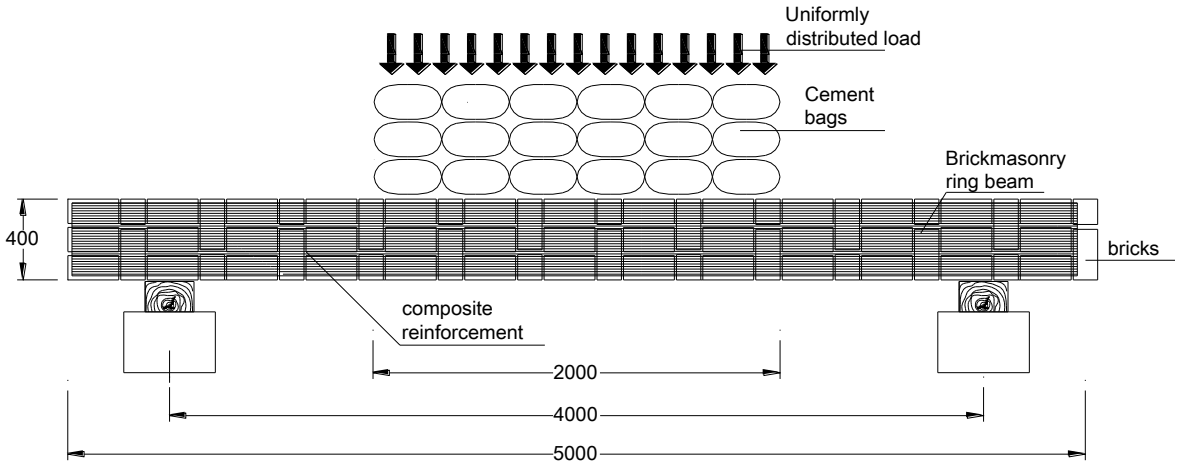

b)

Figure 14. Arrangement of bending test of brickmasonry ring beams: a) bending load applied perpendicularly to the mortar bed joints, b) bending load applied parallel to the mortar bed joints (dimensions in mm).

a) b)

Figure 15. a) Crack pattern produced by self-weight; b) Ring-beam No. P3-U-V after testing.

609

610

611  a)  b)

612 Figure 16. Ring beam No. P5-G33-V: a) under loading, b) detail of the cracks.

613

Figure 17. Test No. P8-G66-H.

619

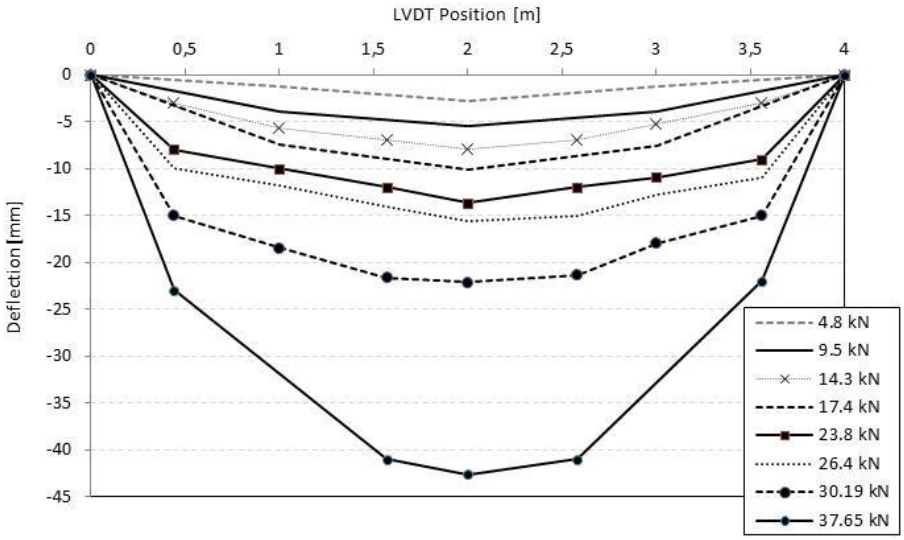

620

621 Figure 18. Deflection vs. position for different load values (L10-G33-H).

622

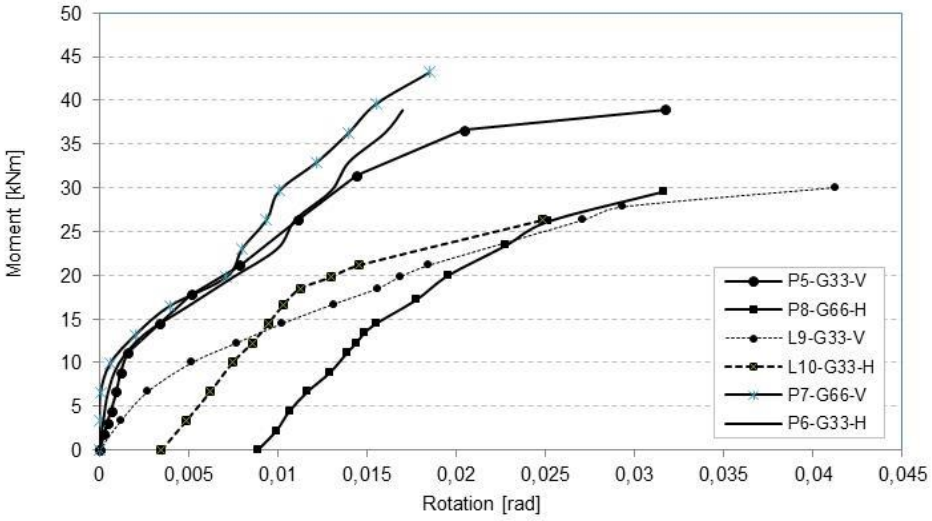

Figure 19. Moment vs. curvature response (for GFRP reinforced beams).

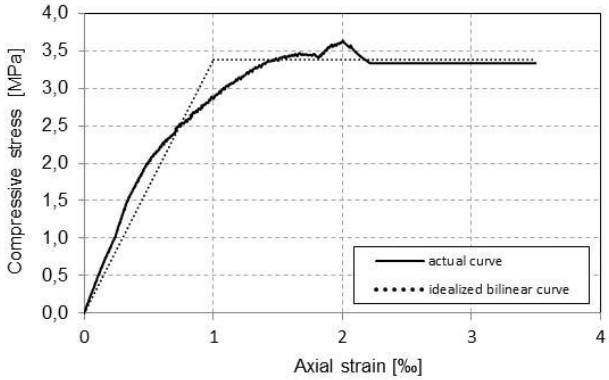

Figure 20. Behavior of stone masonry obtained from compressive tests.

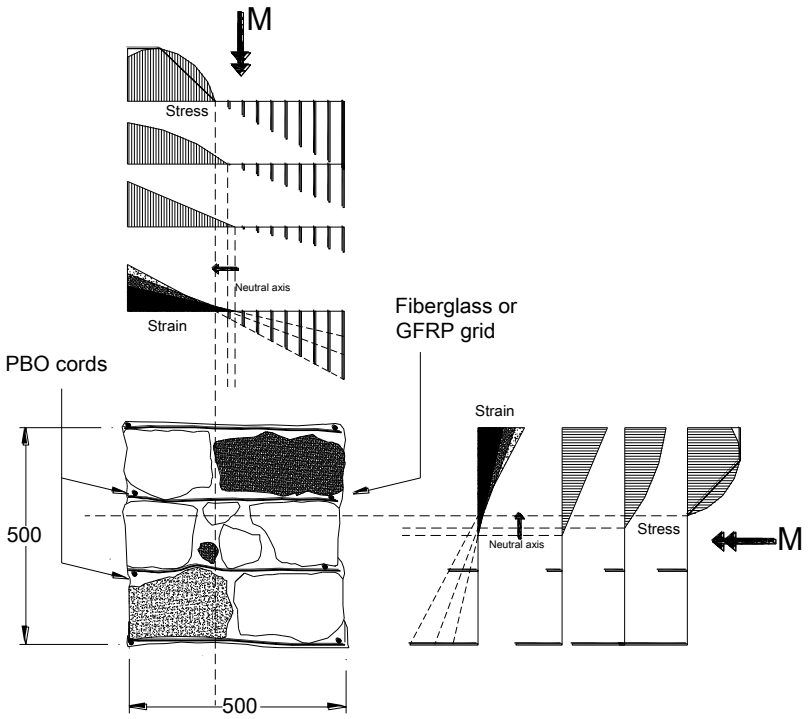

Figure 21. Stress and strain distribution on the stonemasonry cross-section.

642

643

644

645 Table 1. Results of compression tests on mortar samples.

	Sample size	Weight density	Compressive strength	
		[kN/m^3]	Mean	CoV
			[MPa]	[%]
CM	18	18.85	5.99	9.56
MI	6	20.16	10.61	6.32

646 CoV=Coefficient of Variation

647

Table 2. Mechanical properties of PBO cords.

		T cords	U cords
Rope configuration		twisted	unidirectional
Sample size		6	9
Failure tensile load (mean)	[kN]	12.25	11.19
Nominal diameter	[mm]	4	4
Tensile strength (mean)	[MPa]	2923	2661
Young's modulus (mean)	[GPa]	91	250

Table 3. Mechanical properties of welded fiberglass mesh (from producer Data Sheet).

Mesh size	[mm]	12x12
Mesh weight density	[kg/m^2]	0.2
Tensile strength	[MPa]	634
Cross section area	[mm^2/cm]	0.48
Tensile strength	[kN/m]	70
Young modulus	[GPa]	73

661 Table 4. Mechanical properties of GFRP grid.

		Warp	Weft
Tensile strength	[MPa]	634	558
Sample size	[-]	15	13
Cross section	[mm^2]	7.13	8.52
Elongation at failure	[%]	1.60	1.56
Young modulus	[GPa]	39.63	35.72

662

663

664

665

666

667

668 Table 5. Reinforcement's cross sectional areas.

	Beam cross-section [cm^2]	Fiberglass mesh* [mm^2]	PBO cords [mm^2]	GFRP** grid 33x33mm [mm^2]	GFRP** grid 66x66 mm [mm^2]
Stonemasonry beam	2500	96	100.4	171.1	342.2
Brickmasonry beam	1320	-	-	213.9	-

669 * one direction only, ** only warp direction

Table 6. Results of bending tests.

	Bending moment* M_w [kNm]	Max Load [kN]	Bending moment** M_{Load} [kNm]		Total bending moment M_{TOT} [kNm]	
P1-T-V	10.7	16.0	12.00		22.70	
P2-T-H	10.7	9.0	6.75	11.06	17.45	21.76
P3-U-V	10.7	18.0	13.50	(26.76%)	24.20	(13.60%)
P4-U-H	10.7	16.0	12.00		22.70	
P5-G33-V	10.7	56.8	39.75		50.45	
P6-G33-H	10.7	56.6	39.62	38.38	50.32	49.08
P7-G66-V	10.7	62.9	44.03^{+}	(15.26%)	54.73	(11.95%)
P8-G66-H	10.7	43.1	30.14^{+}		40.84	
L9-G33-V	3.86	51.2	35.87	31.33	39.73	35.2
L10-G33-H	3.86	38.3^{+}	26.80^{+}	(20.47%)	30.66	(18.22%)

* produced by the self-weight, ** produced by applied bending loads, $^{+}$ beam failure not reached

CoV in ( )

Table 7. Beam capacity in terms of bending moments: experimental (M_{TOT}) vs. analytical (M_{cal}).

	M_{cal} [kNm]	M_{TOT} [kNm]	$(M_{cal}-M_{TOT})/M_{TOT}$ [%]
P1-T-V	41.49	22.70	+82.8
P2-T-H	36.27	17.45	+107.9
P3-U-V	43.57	24.20	+80.0
P4-U-H	32.42	22.70	+42.8
P5-G33-V	46.14	50.45	-8.5
P6-G33-H	38.75	50.32	-23.0
P7-G66-V	46.14	54.73^{+}	-15.7
P8-G66-H	38.75	40.84^{+}	-5.1
L9-G33-V	49.31	39.73	-24.1
L10-G33-H	43.36	30.66^{+}	+41.4

$^{+}$ beam failure not reached